Advanced Diagnostics Applied to a Laser-Driven Electron-Acceleration Experiment

Andrea Gamucci, Nicolas Bourgeois, Tiberio Ceccotti, Sandrine Dobosz, Pascal D'Oliveira, Marco Galimberti, Jean Galy, Antonio Giulietti, Danilo Giulietti, Leonida A. Gizzi, David J. Hamilton, Luca Labate, Jean-Raphaël Marquès, Pascal Monot, Horia Popescu, Fabrice Réau, Gianluca Sarri, Paolo Tomassini, and Philippe Martin

***Abstract*—In this paper, the interaction of 10-TW laser pulses, focused at moderately relativistic intensity, with a supersonic helium gas-jet has been investigated by varying gas density and jet nozzle. We have successfully tested several advanced diagnostic devices to characterize the plasma and the accelerated electron bunches. Plasma densities have been measured by means of a femtosecond high-resolution interferometer, while the electron beams were analyzed with a stack of radiochromic films, a beam-profile monitor, a magnetic spectrometer, and a nuclear activation setup based on gamma-ray generation via electron bremsstrahlung. We present the results as well as the basic features and relevant details of such diagnostics whose performances can fit a large class of experiments.**

***Index Terms*—Advanced diagnostics, laser–plasma acceleration, plasma measurements.**

I. Introduction

LASER-DRIVEN acceleration of electrons in plasmas was first proposed by Tajima and Dawson [1] in 1979. Table-top laser systems based on the chirped-pulse-amplification (CPA) technique [2], with pulse duration of tens of femtoseconds focused to tight spots capable of producing intensities greater than 10^{18} W/cm^2, have made electron-acceleration experiments possible over a wide range of laser and plasma parameters [3]. In the early experiments, low-quality electron bunches have been accelerated with a nearly 100% energy spread [4]–[7]. A breakthrough from several groups reporting monoenergetic and highly collimated bunches with energies of hundreds of megaelectronvolts gained with a millimetric path in gas-jets [8], [9] demonstrated that the increase of the energy gain, drop of the ΔE/E, and enhancement of the charge of relativistic electron bunches is feasible with a careful control of ultrashort pulses interaction with underdense plasmas. Moreover, with the aid of guiding techniques, energies up to 1 GeV have been achieved in centimeter-scale setups [11], [12].

The major issues still to be pursued are the stability and the operational reproducibility, as well as the tunability of the generated particle bunches in terms of energy, energy spread, collimation, and charge, of such systems. Control of the electron self-injection in the plasma wave has recently been enhanced experimentally with a counterpropagating pulses technique [13]. A key task is the in-depth study of the propagation of high-power laser pulses in plasmas, aimed to optimize the excitement of large-amplitude plasma waves and the injection of electrons in regions with accelerating electric field. The laser pulse that interacts with the target has to be carefully characterized in its spectrum, energy, and duration. Third-order autocorrelators are commonly used to evaluate the power-contrast ratio of the CPA pulse with respect to the pico- and nanosecond pedestals that likely precede it. The focal spot has to be monitored in order to guarantee the cleanest spot shape, as the acceleration process depends critically from the focusing conditions. Spectroscopy and imaging of the transmitted CPA pulse (i.e., in the forward direction, as well as in the backward direction and at 90°) can provide a useful tool in the evaluation of propagation instabilities. The key plasma parameters have to be measured with accuracy: in particular, the electron-density distribution represents one of the most important information concerning the acceleration scenario. Other optical diagnostic tools widely employed are Thomson scattering of laser light, shadowgraphy, and schlieren imaging. Femtosecond interferometry provides a detailed control of the plasma-electron-density profile produced by the ultrashort intense pulse and/or its precursors, as will be described in Section III. Finally, beam-profile monitors, as well as magnetic spectrometers and integrating current transformers,

Manuscript received February 19, 2008; revised April 28, 2008. This work was supported by EU through the Access to Research Infrastructures Activity in the Sixth Framework Program under Contract RII3-CT-2003-506350, Laserlab Europe. The work of A. Gamucci, M. Galimberti, D. Giulietti, L. A. Gizzi, L. Labate, G. Sarri, P. Tomassini, and A. Giulietti was supported in part by the INFN-Pisa Section under the framework of the National PlasmonX Project. The work of M. Galimberti, L. Labate, and G. Sarri is also supported in part by the Italian Ministry of University and Research under the framework of the National Project BLISS.

A. Gamucci, A. Giulietti, L. A. Gizzi, L. Labate, and G. Sarri are with the Intense Laser Irradiation Laboratory, IPCF, CNR, 56124 Pisa, Italy, and also with INFN, Sezione di Pisa, 56100 Pisa, Italy (e-mail: andrea.gamucci@ipcf.cnr.it).

N. Bourgeois and J.-R. Marquès are with the Laboratoire pour l'Utilisation des Lasers Intenses, CNRS UMR 7605, Ecole Polytechnique, 91128 Palaiseau Cedex, France.

T. Ceccotti, S. Dobosz, P. D'Oliveira, P. Monot, H. Popescu, F. Réau, and P. Martin are with CEA-DSM/DRECAM/SPAM, 91191 Gif-sur-Yvette Cedex, France.

M. Galimberti is with the Intense Laser Irradiation Laboratory, IPCF, CNR, 56124 Pisa, Italy, with INFN, Sezione di Pisa, 56100 Pisa, Italy, and also with the Central Laser Facility, Rutherford Appleton Laboratory, OX11 0QX Oxon, U.K.

J. Galy and D. J. Hamilton are with the Institute for Transuranium Elements, 76125 Karlsruhe, Germany.

D. Giulietti is with the Intense Laser Irradiation Laboratory, IPCF, CNR, 56124 Pisa, Italy, with INFN, Sezione di Pisa, 56100 Pisa, Italy, and also with the Dipartimento di Fisica, Università di Pisa, 56100 Pisa, Italy.

P. Tomassini is with the Istituto Nazionale di Fisica Nucleare-MI, 20133 Milan, Italy, and also with IPCF-CNR, 56124 Pisa, Italy.

Color versions of one or more of the figures in this paper are available online at http://ieeexplore.ieee.org.

Digital Object Identifier 10.1109/TPS.2008.2000898

are used to get data on the charge of the electron bunches accelerated in the laser–plasma interaction.

Several phenomena contribute to make the acceleration process poorly predictable. The ones that affect the laser propagation in the plasma are currently extensively studied [17]–[20]. A number of groups have reported the production of relativistic electrons in experiments in which neither the plasma electron density matched the resonant condition for laser-wakefield acceleration (LWFA) nor the laser peak power fulfilled the requirements for the onset of highly nonlinear blowout regime [8], [21]–[24]. The results obtained in those conditions identify an interesting regime to be systematically explored, in which nonlinear phenomena can compensate for the lack of resonant laser/plasma parameters, enabling the production of electron bunches with interesting parameters, including total charge, peak energy, and collimation. The diagnostic tools the experimentalists deal with must then enable a precise tuning of the interaction conditions in terms of laser-focusing conditions and target density.

This paper is organized as follows. Section II presents the setup employed for the experiment, while Section III reports the results of the interferometric data, in addition with a brief description of the deconvolution procedure. In Section IV, the results of electron-bunch characterization are presented, including the results of the successful nuclear photoactivation of a ^{197}Au sample.

II. Experiment

In this paper, we report on the detailed characterization of a "laser-into-gas-jet" experiment, for what concerns the plasma and the electron bunches. We studied the electron acceleration in plasmas driven by a 10-TW laser pulse. The 65-fs pulse was delivered by the UHI10 laser system of the SLIC facility at the CEA Center of Saclay (France) with energy up to 0.8 J at wavelength of 800 nm. The pulse was focused with an $f/5$ off-axis parabolic mirror in a quasi-Gaussian spot of waist $w_0 \approx 6\ \mu$m with peak intensity of $\sim 9 \cdot 10^{18}$ W/cm^2, accounting for a field strength parameter of $a_0 \approx 2$. The laser pulse was focused onto supersonic helium gas-jets flowing out from a circular nozzle, whose diameter was varied for each series of measurements. A variety of nozzle diameters from 0.6 to 10 mm were tested during the experiment. For each nozzle, a variety of helium backing pressures was tested. The supersonic nature of the gas-jet [25] enabled the production of steep gas boundaries.

A set of advanced diagnostic has been employed either to measure the plasma electron density at which the acceleration process took place or the electron-beam characteristics in terms of number, energy spectrum, and angular distribution. High-contrast femtosecond interferometry was employed to measure the plasma-electron-density distribution. The characterization of the electron beams was carried out by making use of four different diagnostics. A Lanex screen was used as beam-profile monitor, while a magnetic spectrometer supplied shot-to-shot the electrons' energy spectrum. The angular distribution and charge of electrons in the bunch were provided by a set of radiochromic foils (RCFs) arranged in a stack with different absorbing materials. Another measurement of the electron-bunch parameter was eventually performed, exploiting the nuclear activation of a ^{197}Au sample by means of the bremsstrahlung photons produced by the electron beams in a suitable converter. The obtained results are consistent with each other and confirm the useful employment of such diagnostics in laser–plasma-based experiments.

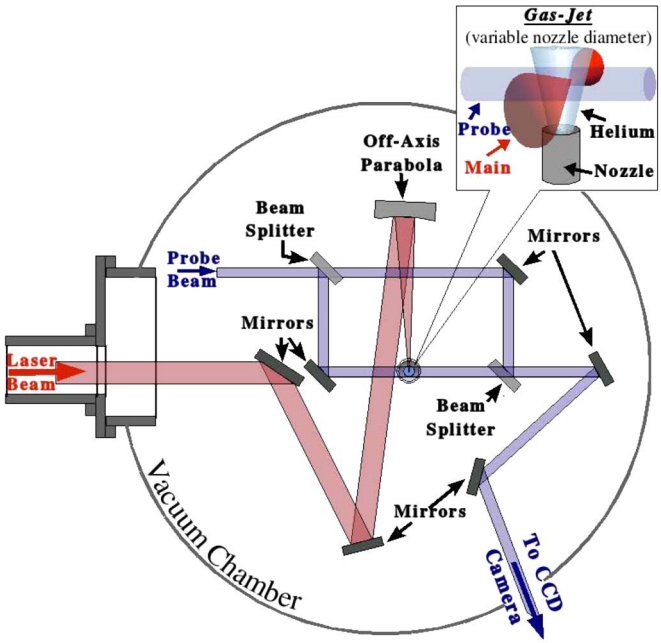

Fig. 1. Setup of the interferometer used for the laser–gas-jet experiment.

III. Characterization of the Plasma: The Femtosecond Interferometry

High-visibility fringe patterns obtained with femtosecond interferometry in the Mach–Zehnder configuration allowed us to control the plasma-electron-density distributions shot-by-shot. The optical probing of the plasma was performed with a fraction of the femtosecond pulse doubled in frequency by a KDP-Type-I 2-mm-thick crystal. The probe beam propagated in a perpendicular direction with respect to the main pulse and the gas flow. By means of an optical delay, it was possible to vary the delay between the arrival of the main CPA pulse and the probe pulse. The layout of the interaction chamber including the interferometer is shown in Fig. 1.

Interferograms have been deconvolved with a fringe-analysis technique that makes use of a continuous-wavelet-transform ridge-extraction algorithm to extract the phase-difference map, evidencing local phase variations with a higher degree of accuracy than other FFT-based techniques [26]. These phase maps are then processed with an algorithm that generalizes the Abel inversion even to distributions that slightly differ from axial cylindrical symmetry by truncating a Legendre polynomial expansion in the azimuthal angle [27]. Electron-density distributions are thus accurately retrieved with low noise. Interferometric patterns have been analyzed with particular attention to some artifacts in phase-difference maps reconstruction that can be connected with the transit time of the probe through

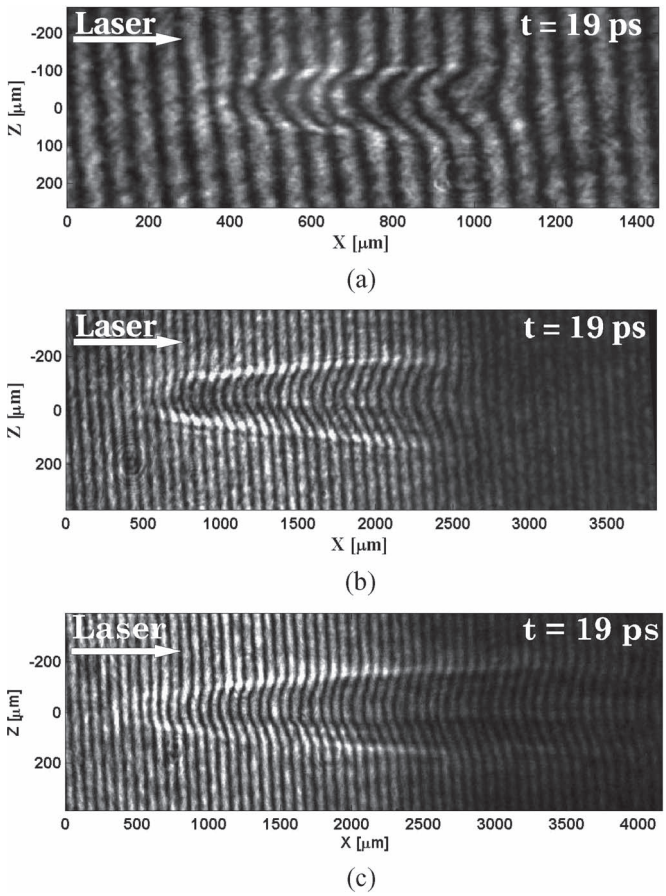

Fig. 2. Interferograms obtained with three different nozzles 19 ps after the plasma formation. (a) 0.6-mm nozzle at 20-bar helium backing pressure. (b) 2-mm nozzle at 8-bar He backing pressure. (c) 4-mm nozzle at 20-bar He backing pressure. The direction of laser propagation is also shown.

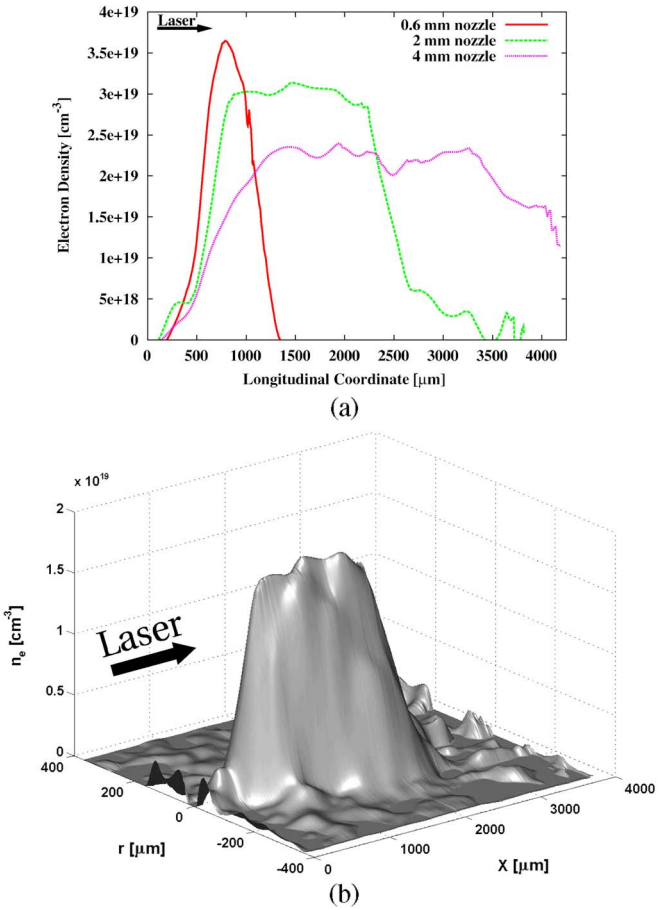

Fig. 3. Deconvolved data obtained with the (solid line) 0.6-, (dashed line) 2-, and (dotted line) 4-mm nozzles. (a) On-axis longitudinal lineout of the plasma electron density for the three cases. (b) Three-dimensional map of the plasma electron density created with the 2-mm nozzle. The direction of laser propagation is also shown.

the plasma [28], [29]. Interferometry gave us a real-time instrument in order to search for the best conditions to achieve efficient electron acceleration, by allowing us to control, in detail, the plasma-electron-density distribution for each gas-jet configuration. In the following, we present data obtained from nozzles with 0.6-, 2-, and 4-mm diameter, since they show interesting features linked with relativistic electron-beam production. Fig. 2 shows the interferograms of the plasmas produced with the three nozzles earlier, in conditions of backing pressure and distance from the orifice selected in order to achieve the best density profile with peak electron density in the range of $2-3\cdot 10^{19}$ cm^{-3}. Fig. 3 shows the longitudinal electron-density lineouts of such plasmas [Fig. 3(a)], as well as the 3-D reconstruction of the electron-density distribution for the 2-mm nozzle [Fig. 3(b)]. In each case, the plasma is probed $\approx$19 ps after its production by the pump pulse.

Concerning the 0.6- and 4-mm gas-jets, the helium backing pressure was 20 bar, and the distance between the laser focus and the nozzle plane was $\approx$1 mm; in the 2-mm-nozzle case, the pressure was 8 bar, and the distance between the laser focus and the nozzle plane was $\approx$0.5 mm.

The electron density has a maximum along the longitudinal axis, since at this time, the shock wave that is hydrodynamically set-on by the laser-energy deposition in the focal region has not yet developed enough to deplete the on-axis region and form a hollow channel [18]. It has to be noted that, with the 2-mm nozzle, the density is almost constant in the high-density plateau. This feature implies that no density fluctuations interfere with laser propagation throughout the plasma. In the case of the 0.6-mm nozzle, the electron density does not reach a complete plateau condition on the axis but the density profile is suitably smooth with a density variation of $\approx$20% along 0.5 mm. With the 4-mm nozzle, the density shows some modulations in the plateau region, accounting for variations of less than 15%, while in the region of laser exit, the density lowers smoothly up to half of its plateau value, because of the defocusing of the laser beam through the gas.

IV. Characterization of the Accelerated Electron Bunches

As the interferometric data clearly show, the electron density we have used is well above $7\cdot 10^{17}$ cm^{-3} as requested for the 65-fs laser pulse to resonantly excite high-amplitude plasma waves within the LWFA scheme. However, also such "high-density" conditions have been proved to be suitable for the production of relativistic electron bunches [8], [10], [20], [22]. We produced, in fact, high-charge electron bunches in this conditions. In the following, we present experimental data

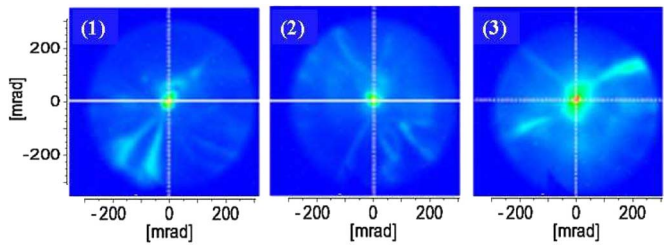

Fig. 4. Electron spots recorded by the beam-profile monitor for laser interaction with the 2-mm-diameter gas-jet.

on electron acceleration obtained with the interaction of the focused laser pulse with 2- and 4-mm He gas-jet, as these configurations gave the most interesting results.

A. Beam-Profile Monitor and Magnetic Spectrometer

The first real-time measurement (useful also for the fine tuning of the experiment) was provided by a beam-profile monitor, made up of a scintillating Lanex plate placed 44 mm behind the focal point and screened from laser light, X-rays, and low-energy electrons by a 300-μm Cu foil. With this technique, a pointing stability of less than 100 mrad of the fairly collimated electron bunches was revealed by a large number of patterns, some of which are shown in Fig. 4.

It resulted that the mean divergence angle of the central feature with single-shot exposition was approximately 30-mrad FWHM. Furthermore, some radial structures are shown in Fig. 4 (whose patterns varied shot-to-shot), whose nature will be discussed in Section IV-B.

The spectrum of the accelerated electrons was firstly provided shot-to-shot by the magnetic spectrometer. The magnetic spectrometer consisted of a ~1-T 1.5-mm-aperture permanent magnet put between the electron source and the Lanex screen. The output of the spectrometer was imaged by the Lanex plate. With this detector, it has been possible to monitor shot-by-shot the high-energy component of the generated electrons, in order to optimize the acceleration process by varying the focusing conditions and nozzle aperture. The data provided by the magnetic spectrometer for both 2- and 4-mm nozzles show the presence of high-energy peaks in electron spectra, at energies in the range from 10 to 45 MeV. Fig. 5 shows a spectrum obtained with the 2-mm nozzle, in which energy peaks from 15 up to 38 MeV are clearly visible.

Due to the nonlinear nature of the effects that onset in the acceleration process, we found shot-to-shot variations in the energy spectrum of the electrons; however, high-charge bunches are present in almost all the shots, with energy peaked in the range of 10–40 MeV.

B. SHEEBA Stack of Radiochromic Films

High-energy electrons accelerated in the laser–plasma interaction have been characterized in number, spectrum, and angular distribution using an RCF-based detector named spatial high-energy electron-beam analyzer (SHEEBA) [30]. It consists of an array of RCFs (specifically Gafchromic HD810 and MD55) separated from each other by absorbers of different

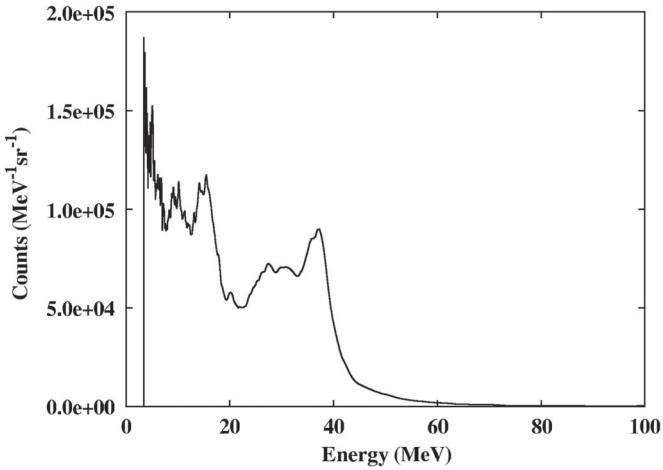

Fig. 5. Electron spectrum obtained with the magnetic spectrometer.

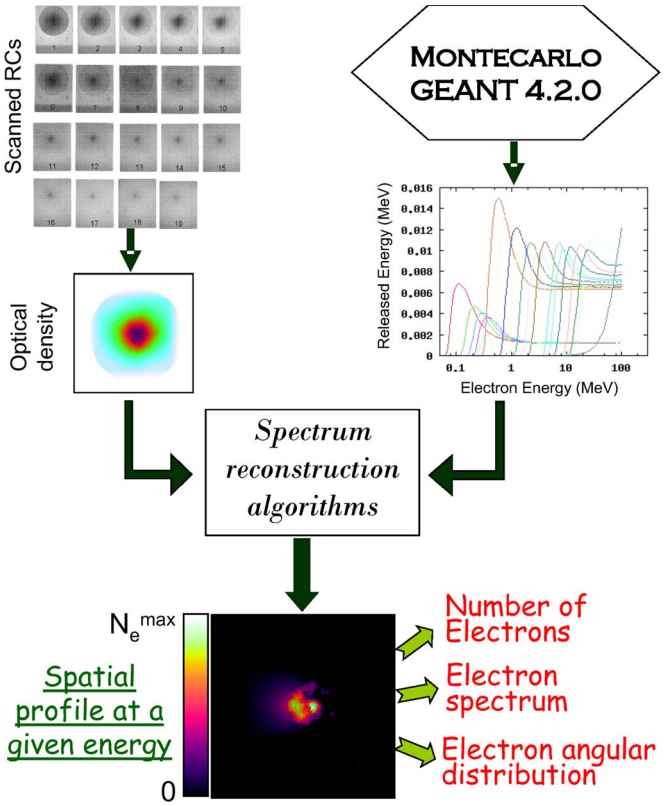

Fig. 6. Schematic of the analysis procedure to evaluate the key parameters of the electron bunches that impinge on the SHEEBA detector. As a result, the spatial profiles at given incident electron energies are retrieved.

thickness and materials: Mylar foils, aluminum, iron, and lead. The operational principle of the SHEEBA detector is the same as for a sampling calorimeter. RCFs are sensitive to charged particles; in particular, the change in their optical density after exposure is proportional to the released energy (absorbed dose). The detector is able to provide both the angular distribution, due to its 2-D feature (no pinholes or slit are needed), and the spectrum of the incoming electron bunch. Indeed, the higher the kinetic energy of a given particle, the farther the RCF layer its energy is deposited in. Thus, once the following steps are performed: 1) the optical density versus dose for a single RCF

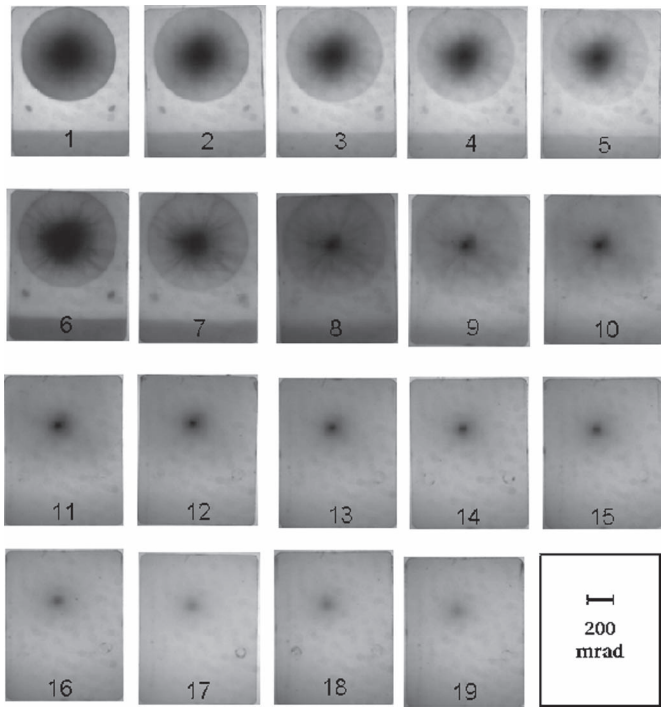

Fig. 7. Raw data extracted from the SHEEBA device after ten laser shots. Layer number increases with distance from the electron source.

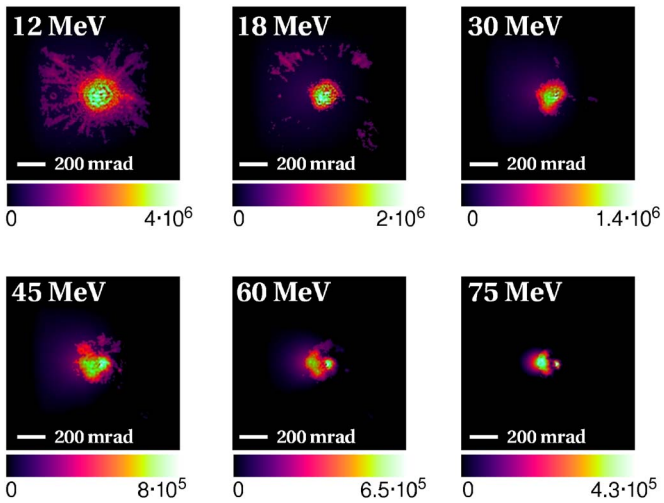

Fig. 8. Spatial profiles at different energies of the electron bunches produced by the same ten consecutive laser shots as for pattern of Fig. 7.

layer is known and 2) the energy released in each layer of the actual RCFs-absorbers stack is calculated for a set of discrete kinetic-energy points, then the spectrum of the incoming bunch can be retrieved by means of an iterative algorithm [30]. In particular, step 2) can be carried out by means of Monte Carlo simulations of the electron transport inside the detector. The whole analysis procedure is schematically shown in Fig. 6.

The optical-density distributions of the scanned images of the RCFs are convolved with the results of a Monte Carlo simulation performed with a code based on CERN GEANT4 libraries [31] to reconstruct the spectrum of the incoming electrons. The Monte Carlo calculation simulates the energy density released in each radiochromic layer by a monochromatic beam of electrons impinging on the device.

As an example, a set of RCFs after exposure to the electron flux generated by the interaction of the laser pulse with the 4-mm-diameter gas-jet is shown in Fig. 7. The patterns were produced by the action of ten consecutive laser shots.

The raw data of Fig. 7 present, even from a qualitative point of view, some features that deserve an in-depth analysis. First, it is possible to notice in RCFs up to layer #10 radial structures similar to the ones provided by the beam-profile monitor (see Fig. 4). From the 11th layer onwards, the patterns show basically only a spot in the center. It comes out that the radial structures in the first layers are due to some low-energy electron populations. In fact, they are found to disappear in the subsequent layers on, since only the high-energy electrons survive beyond the absorber materials. The central spot present in all the RCFs is then the footprint of high-energy, well-collimated, and stable electron bunches integrated over ten laser shots. The pointing position of the electron beams is found to remain very constant, leading to an angular divergence of less than 100 mrad for the ten shots integration. If compared to the single-shot Lanex data, this result is a further convalidation of the electron-beam quality.

Fig. 8 shows six images of electron spatial profiles at different energies, ranging from 12 to 75 MeV, obtained after the processing of the RCFs of Fig. 7.

Notice that, in the lower energy profiles, the radial structures already evidenced in the Lanex patterns (see Fig. 4) are recognizable, while the central spot is still quite large with more than 200-mrad divergence. As the energy increases, the structures drop away, and the more collimated low-divergence spot remains at the center of the image. It is then clear that the electron population of lower energy is less collimated and partially originated by unstable regions in the laser–plasma interaction. For this particular series of shots, the analysis reveals at high energy the presence of at least two spatially separated lobes. These distinct components are probably due to electron bunches produced in different laser shots (among the ten shots) and with a slightly different pointing direction. An angular divergence of less than 50 mrad is retrieved for most of the peaks. The good collimation and the stability of the electron bunches is thus confirmed by the SHEEBA data.

C. Photonuclear Activation of Radioisotopes

Photoactivation of a nuclear sample has also been used in the experiment, in order to obtain further reliable data on the electron-beam flux. The employed nozzle diameter was 4 mm in this case. The laser focal point was located 35-mm upstream of the tantalum, while the Au sample was put 50 mm behind the Ta converter. The reaction of interest in our tests was $^{197}\mathrm{Au}(\gamma,\mathrm{n})^{196}\mathrm{Au}$. The cross section for the (γ,n) reaction is indeed relatively large for photon energies around 10–15 MeV, due to the presence of a resonance in the nuclear photoabsorption amplitude, known as the giant dipole resonance [32]. The photonuclear reactions allowed us to measure the number of useful $(\mathrm{E} > 3$ MeV$)$ electrons with a three-step process. First, the irradiation of a gold foil by the flux of photons originating by bremsstrahlung radiation of laser–gas-jet

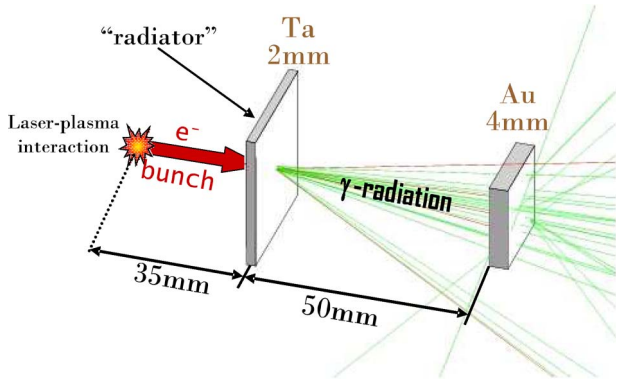

Fig. 9. Setup of the arrangement of converter and sample slabs for nuclear-activation tests.

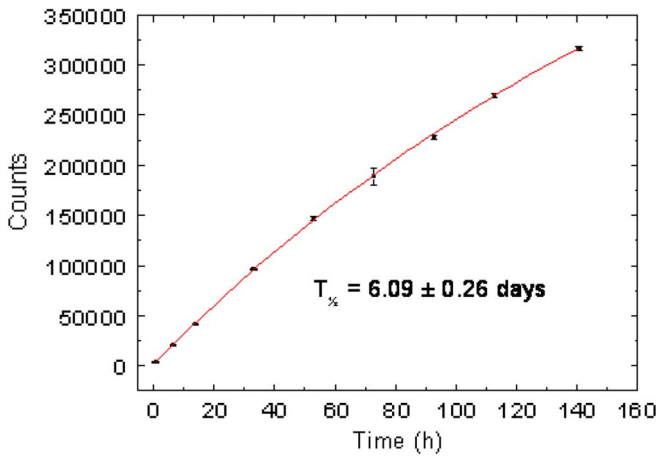

Fig. 10. Counts from ^{196}Au decays as a function of time. The half-life $t_{1/2}$ resulting from the fit of the data agrees with nuclear databases value.

accelerated electrons in a suitable high-Z converter (tantalum in our case). Then, the radioactivity of the activated sample has been measured with a high-purity germanium detector via calibrated gamma spectroscopy. Finally, the absolute number of incident bremsstrahlung photons and beam electrons has been retrieved from the experimental data and the predictions of a dedicated Monte Carlo code. The schematic layout of the setup employed for the photoactivation measurements is shown in Fig. 9.

The sample has been irradiated with 106 laser shots. The postprocessing was based on the two lines at 333 and 355 keV emitted by the decay of ^{196}Au. As a self-consistency check, the half-life was determined from both gamma lines to be (6.09 $\pm$ 0.26) days, which is in good agreement with nuclear databases value for the emission of the two primary photons for this radionuclide [33]. The obtained decay curve is shown in Fig. 10.

The last step in the analysis procedure concerns the calculation of the bremsstrahlung flux that gave rise to the retrieved number of produced ^{196}Au nuclei via (γ, n) reactions. From the bremsstrahlung flux, it is then possible to calculate the corresponding electron-beam flux, once the relative electron-beam energy spectrum and the differential cross section for the $^{197}\mathrm{Au}(\gamma, \mathrm{n})^{196}$Au reaction are known. To do so, GEANT4 [31] Monte Carlo package was used, taking into account the experimental geometry, the relative electron-energy spectrum and divergence, and the gold photonuclear cross section as inputs of the code. The electron spectrum was retrieved with the magnetic spectrometer.

As a result, a number of electrons of $(3.15 \pm 0.13) \cdot 10^{10}$ per laser shot with energy higher than 3.4 MeV was found. It is worth noting that the number of electrons with energy higher than 3.2 MeV retrieved with the SHEEBA detector was $\sim 3 \cdot 10^{11}$ for a cumulation of ten laser shots, and thus, the agreement between the two results is very good. These values testify the efficiency we reached in the production of relativistic electron bunches.

V. Conclusion

From the experimental point of view, the production of high-energy electrons in laser–plasma interactions has been fully characterized in its key parameters. The relativistic electron bunches we produced were described in terms of spectrum, number, and angular divergence. This was possible owing to suitable diagnostics. We have shown how the use of high-contrast femtosecond interferometry, in addition to a novel fringe-deconvolution technique, can provide electron-density profiles with high-degree of accuracy. A dedicated algorithm accounts even for nonaxisymmetric plasma distributions. Collimation, pointing stability, number, and spectrum of the accelerated electrons have been carefully characterized with the employment of several independent diagnostics: a Lanex beam-profile monitor, a magnetic spectrometer, the SHEEBA array of RCFs, and a setup for nuclear photoactivation. A gold sample has been irradiated with the bremsstrahlung photons generated by the electrons in a tantalum converter, and the measured activity was used, together with a Monte Carlo code, to evaluate the number of the (γ, n) reactions and thus the number of the electrons in the high-current accelerated beams. There is a very good agreement in the total number of accelerated electrons between the radiochromic and nuclear measurements.

References

[1] T. Tajima and J. Dawson, "Laser electron accelerator," *Phys. Rev. Lett.*, vol. 43, no. 4, pp. 267–270, 1979.
[2] D. Strickland and G. Mourou, "Compression of amplified chirped optical pulses," *Opt. Commun.*, vol. 56, no. 3, pp. 219–221, 1985.
[3] E. Esarey, P. Sprangle, J. Krall, and A. Ting, "Overview of plasma-based accelerator concepts," *IEEE Trans. Plasma Sci.*, vol. 24, no. 2, pp. 252–288, Apr. 1996.
[4] M. Everett, A. Lal, D. Gordon, C. Clayton, K. Marsh, and C. Joshi, "Trapped electron acceleration by a laser-driven relativistic plasma wave," *Nature*, vol. 368, no. 6471, pp. 527–529, Apr. 1994.
[5] A. Modena, Z. Najmudin, A. E. Dangor, C. E. Clayton, K. Marsh, C. Joshi, V. Malka, C. Darrow, C. Danson, D. Neely, and F. Walsh, "Electron acceleration from the breaking of relativistic plasma waves," *Nature*, vol. 377, no. 6550, pp. 606–608, 1995.
[6] A. Ting, C. Moore, K. Krushelnick, C. Manka, E. Esarey, P. Sprangle, R. Hubbard, H. Burris, R. Fischer, and M. Baine, "Plasma wakefield generation and electron acceleration in a self-modulated laser wakefield accelerator experiment," *Phys. Plasmas*, vol. 4, no. 5, pp. 1889–1899, May 1997.
[7] V. Malka, S. Fritzler, E. Lefebvre, M. B. Aleonard, J. Chambaret, J. Chemin, K. Krushelnick, G. Malka, S. P. D. Mangles, Z. Najmudin, M. Pittman, J. Rousseau, J. Scheurer, B. Walton, and A. E. Dangor, "Electron acceleration by a wake field forced by an intense ultrashort laser pulse," *Science*, vol. 298, no. 5598, pp. 1596–1600, 2002.

[8] S. P. D. Mangles, C. Murphy, Z. Najmudin, A. G. R. Thomas, J. Collier, A. E. Dangor, E. Divall, P. Foster, J. Gallacher, C. J. Hooker, D. A. Jaroszynski, A. J. Langley, W. Mori, P. A. Norreys, F. Tsung, R. Viskup, B. Walton, and K. Krushelnick, "Monoenergetic beams of relativistic electrons from intense laser–plasma interactions," *Nature*, vol. 431, no. 7008, pp. 535–538, 2004.

[9] J. Faure, Y. Glinec, S. Pukhov, A. Kiselev, S. Gordienko, E. Lefebvre, J. Rousseau, F. Burgy, and V. Malka, "A laser–plasma accelerator producing monoenergetic electron beams," *Nature*, vol. 431, no. 7008, pp. 541–544, 2004.

[10] C. Geddes, C. Toth, J. van Tilborg, E. Esarey, C. Schroeder, D. Bruhwiler, C. Nieter, J. Cary, and W. Leemans, "High-quality electron beams from a laser wakefield accelerator using plasma-channel guiding," *Nature*, vol. 431, no. 7008, pp. 538–541, 2004.

[11] W. Leemans, B. Nagler, A. Gonsalves, C. Toth, K. Nakamura, C. Geddes, E. Esarey, C. Schroeder, and S. M. Hooker, "GeV electron beams from a centimetre-scale accelerator," *Nat. Phys.*, vol. 2, pp. 696–699, 2006.

[12] S. Karsch, J. Osterhoff, A. Popp, T. P. Rowlands-Rees, Z. Major, M. Fuchs, B. Marx, R. Horlein, K. Schmid, L. Veisz, S. Becker, U. Schramm, B. Hidding, G. Pretzler, D. Habs, F. Gruner, F. Krausz, and S. M. Hooker, "GeV/scale electron acceleration in a gas-filled capillary discharge waveguide," *New J. Phys.*, vol. 9, no. 11, p. 415, 2007.

[13] J. Faure, C. Rechatin, A. Norlin, A. Lifschitz, Y. Glinec, and V. Malka, "Controlled injection and acceleration of electrons in plasma wakefields by colliding laser pulses," *Nature*, vol. 444, no. 7120, pp. 737–739, 2006.

[14] J. Rosenzweig, "Nonlinear plasma dynamics in the plasma wakefield accelerator," *Phys. Rev. Lett.*, vol. 58, no. 6, pp. 555–558, Feb. 1987.

[15] P. Sprangle, E. Esarey, and A. Ting, "Nonlinear theory of intense laser–plasma interactions," *Phys. Rev. Lett.*, vol. 64, no. 17, pp. 2011–2014, 1990.

[16] P. Sprangle, J. Krall, and E. Esarey, "Hose-modulation instability of laser pulses in plasmas," *Phys. Rev. Lett.*, vol. 73, no. 26, pp. 3544–3547, 1994.

[17] A. Giulietti, P. Tomassini, M. Galimberti, D. Giulietti, L. A. Gizzi, P. Koester, L. Labate, T. Ceccotti, P. D'Oliveira, T. Auguste, P. Monot, and P. Martin, "Prepulse effect on intense femtosecond laser pulse propagation in gas," *Phys. Plasmas*, vol. 13, no. 9, p. 093 103, 2006.

[18] A. Gamucci, M. Galimberti, D. Giulietti, L. A. Gizzi, L. Labate, C. Petcu, P. Tomassini, and A. Giulietti, "Production of hollow cylindrical plasmas for laser guiding in acceleration experiments," *Appl. Phys. B, Photophys. Laser Chem.*, vol. 85, no. 4, pp. 611–617, 2006.

[19] S. Deng, C. D. Barnes, C. E. Clayton, C. O'Connell, F. J. Decker, R. A. Fonseca, C. Huang, M. J. Hogan, R. Iverson, D. K. Johnson, C. Joshi, T. Katsouleas, P. Krejcik, W. Lu, W. B. Mori, P. Muggli, E. Oz, F. Tsung, D. Walz, and M. Zhou, "Hose instability and wake generation by an intense electron beam in a self-ionized gas," *Phys. Rev. Lett.*, vol. 96, no. 4, p. 045 001, 2006.

[20] S. P. D. Mangles, A. G. R. Thomas, O. Lundh, F. Lindau, M. Kaluza, A. Persson, C.-G. Wahlström, K. Krushelnick, and Z. Najmudin, "On the stability of laser wakefield electron accelerators in the monoenergetic regime," *Phys. Plasmas*, vol. 14, no. 5, p. 056 702, 2007.

[21] N. Hafz, M. Hur, G. Kim, C. Kim, I. Ko, and H. Suk, "Quasimonoenergetic electron beam generation by using a pinholelike collimator in a self-modulated laser wakefield acceleration," *Phys. Rev. E, Stat. Phys. Plasmas Fluids Relat. Interdiscip. Top.*, vol. 73, no. 1, p. 016 405, 2006.

[22] B. Hidding, K. U. Amthor, B. Liesfeld, H. Schwoerer, S. Karsch, M. Geissler, L. Veisz, K. Schmid, J. Gallacher, S. Jamison, D. A. Jaroszynski, G. Pretzler, and R. Sauerbrey, "Generation of quasimonoenergetic electron bunches with 80-fs laser pulses," *Phys. Rev. Lett.*, vol. 96, no. 10, p. 105 004, 2006.

[23] T. Hosokai, K. Kinoshita, T. Ohkubo, A. Maekawa, M. Uesaka, A. Zhidkov, A. Yamazaki, H. Kotaki, M. Kando, K. Nakajima, S. V. Bulanov, P. Tomassini, A. Giulietti, and D. Giulietti, "Observation of strong correlation between quasimonoenergetic electron beam generation by laser wakefield and laser guiding inside a preplasma cavity," *Phys. Rev. E, Stat. Phys. Plasmas Fluids Relat. Interdiscip. Top.*, vol. 73, no. 3, p. 036 407, 2006.

[24] K. Koyama, M. Adachi, E. Miura, S. Kato, S. Masuda, T. Watanabe, A. Ogata, and M. Tanimoto, "Monoenergetic electron beam generation from a laser–plasma accelerator," *Laser Part. Beams*, vol. 24, no. 1, pp. 95–100, 2006.

[25] S. Semushin and V. Malka, "High density gas jet nozzle design for laser target production," *Rev. Sci. Instrum.*, vol. 72, no. 7, pp. 2961–2965, 2001.

[26] P. Tomassini, A. Giulietti, L. A. Gizzi, M. Galimberti, D. Giulietti, M. Borghesi, and O. Willi, "Analyzing laser plasma interferograms with a continuous wavelet transform ridge extraction technique: The method," *Appl. Opt.*, vol. 40, no. 35, pp. 6561–6568, 2001.

[27] P. Tomassini and A. Giulietti, "A generalization of Abel inversion to non-axisymmetric density distribution," *Opt. Commun.*, vol. 199, no. 1–4, pp. 143–148, 2001.

[28] M. Galimberti, "Probe transit effect in interferometry of fast moving samples," *J. Opt. Soc. Amer. A, Opt. Image Sci.*, vol. 24, no. 2, pp. 304–310, 2007.

[29] L. A. Gizzi, M. Galimberti, A. Giulietti, D. Giulietti, P. Koester, L. Labate, P. Tomassini, P. Martin, T. Ceccotti, P. D'Oliveira, and P. Monot, "Femtosecond interferometry of propagation of a laminar ionization front in a gas," *Phys. Rev. E, Stat. Phys. Plasmas Fluids Relat. Interdiscip. Top.*, vol. 74, no. 3, p. 036 403, 2006.

[30] M. Galimberti, A. Giulietti, D. Giulietti, and L. A. Gizzi, "SHEEBA: A spatial high energy electron beam analyzer," *Rev. Sci. Instrum.*, vol. 76, no. 5, p. 053 303, 2005.

[31] S. Agostinelli *et al.*, "GEANT4—A simulation toolkit," *Nucl. Instrum. Methods Phys. Res. A, Accel. Spectrom. Detect. Assoc. Equip.*, vol. 506, no. 3, pp. 250–303, 2003.

[32] J. Speth and A. Van Der Woude, "Giant resonances in nuclei," *Rep. Prog. Phys.*, vol. 44, no. 7, pp. 719–786, 1981.

[33] *IAEA Photonuclear Data Library*. [Online]. Available: http://www-nds.iaea.org/photonuclear

Andrea Gamucci was born in San Miniato, Pisa, Italy, in 1980. He received the B.S. degree in physics and the M.S. degree from the University of Pisa, Pisa, in 2003 and 2005, respectively. He is currently working toward the Ph.D. degree in applied physics at the University of Pisa and in the Intense Laser Irradiation Laboratory, IPCF, CNR, Pisa.

He has been involved in experiments concerning both the characterization (by means of optical diagnostics) of plasmas suitable for electron acceleration driven by ultraintense laser pulses and high-energy electrons production.

Nicolas Bourgeois, photograph and biography not available at the time of publication.

Tiberio Ceccotti, photograph and biography not available at the time of publication.

Sandrine Dobosz, photograph and biography not available at the time of publication.

Pascal D'Oliveira, photograph and biography not available at the time of publication.

Marco Galimberti, photograph and biography not available at the time of publication.

Jean Galy received the degree in physics and neutron physics in Marseille, France, and the Ph.D. degree on the measurement of the fission products of ^{233}U in a fast neutron flux in Sweden.

He was with the CEA Cadarache. He joined the European Commission-Joint Research Centre at the Institute for Transuranium Elements, Kalrsruhe, Germany, where he has been a Scientific Officer since 2000, sharing his time between the development of the software package Nucleonica and laser-induced nuclear-reaction experiments. In 2007, he was with the "Nuclear Safeguard and Security" Unit.

Antonio Giulietti, photograph and biography not available at the time of publication.

Danilo Giulietti received the degree in physics from Pisa University, Pisa, Italy, in 1973 and the Ph.D. degree from Scuola Normale di Pisa, Pisa, in 1979.

Since 1973, he has been continually developing the scientific and teaching activity at the Physics Department "E. Fermi," Pisa University, where he is currently an Associated Professor and Lecturer of classical electrodynamics and quantum optics. The research fields in which he has been involved are in the atomic and molecular physics, electron and nuclear magnetic resonance, thermal radiation, phase transitions, laser-produced plasmas, physics of the inertial confinement fusion, lasers, holography and interferometry, ultrafast electron optics, pulsed X-ray sources and their applications, X-ray spectroscopy, femtosecond lasers, laser–matter interaction at relativistic intensities, and particle acceleration in the plasmas. He is the Author of about 120 publications in international journals and more than 220 communications in national and internationals congresses, some of them as invited talks. He has been in charge of the management of some scientific international initiatives and the Chair of international congresses devoted to the topics of his research activity. Due to his activity in the field of particle acceleration in the plasmas, he is associated to the Istituto Nazionale di Fisica Nucleare (INFN). He is the National Representative of the INFN Strategic Project PLASMONX: plasma acceleration and monochromatic tunable X-ray radiation.

Leonida A. Gizzi was born in Telese Terme, Italy, in 1965. He received the Master "Laurea" degree in physics from the University of Pisa, Pisa, Italy, in 1989 and the Ph.D. degree in physics from the Imperial College of Science, Technology and Medicine, London, U.K., in 1994.

He is an Experimental Physicist working in the field of high-power laser–plasmas. In 1995, he was a Research Staff Member of the experimental astrophysics X-ray group in ITESRE, National Research Council (CNR), Bologna, Italy. Since 1997, he has been IFAM-CNR, currently IPCF-CNR, Pisa, where he is currently a Senior Researcher and Head of the unit of High Field Photonics. Since 2003, he has also been an Associate Researcher of the Italian National Institute of Nuclear Physics, Sezione di Pisa, Pisa. He is the coauthor of more than 90 refereed publications.

David J. Hamilton, photograph and biography not available at the time of publication.

Luca Labate received the Ph.D. degree in physics in 2004.

He is currently a Researcher with the Intense Laser Irradiation Laboratory, IPCF, CNR, Pisa, Italy. He is an Experimentalist working in the field of (ultra)short and (ultra)intense laser–matter interaction, ranging from particle acceleration to ICF.

Jean-Raphaël Marquès, photograph and biography not available at the time of publication.

Pascal Monot, photograph and biography not available at the time of publication.

Horia Popescu, photograph and biography not available at the time of publication.

Fabrice Réau, photograph and biography not available at the time of publication.

Gianluca Sarri was born in 1983. He received the B.S. degree in physics and the M.S. degree in applied physics from the Physics Department "E. Fermi," Pisa University, Pisa, Italy, in 2004 and 2007, respectively. He has been working toward the Ph.D. degree in plasma physics in the Center For Plasma Physics, Queen's University Belfast, Belfast, U.K., since September 2007.

Paolo Tomassini received the degree in physics from the Università di Pisa, Pisa, Italy, in 1993, with a thesis on quantum gravity, and the Ph.D. degree in physics from the University of Genoa, Genoa, Italy, in 1997, with a thesis in field theory applied to turbulence.

Since then, he was a Researcher with the Istituto Nazionale di Fisica Nucleare (INFN) spin-off and an Associate Researcher with the ILIL-CNR Group, Pisa. Since 2007, he has been with the Milan Section of INFN. He is also currently with IPCF-CNR, Pisa. Since 2005, he has been the Coordinator of the PLASMONX package "laser–plasma electron acceleration." His research interests include laser–plasma interactions, e-beam acceleration, X-ray production, and, recently, on FEL physics.

Philippe Martin, photograph and biography not available at the time of publication.